Implementing entorhinal grid fields in biophysical neuronal models

Michiel Remme, Mate Lengyel, Boris Gutkin

IMPLEMENTING ENTORHINAL GRID FIELDS IN BIOPHYSICAL NEURONAL MODELS

Michiel W.H. Remme
Group for Neural Theory, Département d'Études Cognitives
École Normale Supérieure, 3 rue d'Ulm, 75005 Paris, France
email: michiel.remme@ens.fr

Máté Lengyel
Computational and Biological Learning Lab, Department of Engineering
University of Cambridge, Trumpington Street, Cambridge CB2 1PZ, United Kingdom
email : m.lengyel@eng.cam.ac.uk

Boris S. Gutkin
Group for Neural Theory, Département d'Études Cognitives
École Normale Supérieure, 3 rue d'Ulm, 75005 Paris, France
email: boris.gutkin@ens.fr

ABSTRACT
The responses of rat medial entorhinal cortical neurons form characteristic grid patterns as a function of the animal's position. A recent model of grid fields proposes a mechanism based on intrinsic single cell properties. It relies on interference patterns emerging from multiple distinct and independent oscillations maintained in the dendritic tree of the cell. Here we examine the requirements necessary to implement this idealized mechanism in a biophysically realistic model. We find that appropriate grid field-formation by a single cell is exquisitely sensitive to intra-dendritic interactions. Mathematical analysis shows how these effects depend on properties of the dendritic oscillators and the (active) membrane segments that connect them. This work gives explicit requirements for a single cell implementation of grid-field activity.

KEY WORDS
grid cell, subthreshold oscillations, interference model

1 Introduction

The responses of rat medial entorhinal cortical neurons form characteristic grid patterns as a function of the animal's position [1]. The hexagonal grid patterns remain stable over long periods and even persist in the dark. A recent phenomenological model of grid fields proposes a mechanism based on intrinsic single cell properties [2, 3]. The mechanism relies on interference patterns emerging from multiple distinct membrane potential oscillations being maintained in a single dendritic tree. Indeed, stellate cells from the entorhinal cortex show intrinsic subthreshold membrane potential oscillations [4, 5] – generally thought to result from the interaction between a persistent sodium current I_{NaP} and the hyperpolarization activated inward current I_h [4, 6]. In the interference model, the frequencies of the dendritic oscillators are modulated by inputs that signal the animal's head-direction and running speed. The amplitude of the interference patterns at the soma subsequently determines the somatic spiking of the neuron. Besides grid field activity, the model can also successfully account for the phase precession that these cells show [7]. Also, the model agrees with *in vitro* evidence that shows a correlation between the intrinsic oscillator frequencies and the grid field spacing and sizes which increase along the dorsal-to-ventral axis of the entorhinal cortex as predicted by the interference model [8].

However, the current description of the interference model is highly idealized and holds many assumptions. First, the oscillators are described by sinusoids and the interference patterns emerge from both summating and multiplying the different oscillator voltages. Furthermore, the model needs identical oscillators with oscillation frequencies that are linearly related to the speed in a particular direction. A key requirement for the model is that different oscillators within one cell are independent, i.e. they do not affect each other's phase. However, as the oscillators need to produce interference patterns at the soma, one expects that they will also interact with each other. Previous results hint that interactions between the oscillators will typically lead to phase-locking which would potentially disrupt the hexagonal grid field patterns.

Here we examine the requirements necessary to implement the idealized sinusoid-interference mechanism in a biophysical model that sustains intrinsic dendritic oscillations.

2 Results

2.1 Mathematical Analysis

First we carry out a mathematical analysis to determine how fast phase-locking of dendritic oscillators occurs as a function of the oscillator and cable properties. Consider a system of two identical oscillators that are coupled via a (quasi-active) cable of length l cm, with oscillator $i = 1,2$ located at $x = 0$ and $x = l$, respectively (figure 1A). The membrane potential $V_i(t)$ (in millivolts) of each oscillator is described by a sinusoidal function:

$$V_i(t) = A\cos(\omega(t+\theta_i)), \tag{1}$$

where A is the amplitude (in millivolts), ω is the angular frequency, and θ_i is the phase shift of oscillator i. We want to determine how the oscillators influence each other's phase. Assuming weak coupling between the oscillators (i.e. the interactions only affect the oscillators' phases) we can write the changes in the phase shifts of the oscillators as

$$\dot{\theta}_i = \varepsilon Z(t) \cdot p_i(t), \tag{2}$$

where the positive parameter $\varepsilon \ll 1$, and $Z(t)$ is the infinitesimal phase response function (iPRC) which is identical for both oscillators. It describes the change of the oscillator's phase shift in response to an infinitesimally small and short perturbation at a particular phase [9]. The perturbations $p_i(t)$ result from the axial currents that flow between the cable and oscillator i. The passive properties of the cable are determined by a membrane time constant τ (in milliseconds), a leak reversal potential E_L (in millivolts), and a length constant λ (in centimeters), giving the cable an electrotonic length $L = l/\lambda$. The cable also expresses a voltage-dependent conductance with reversal potential E_m. The dynamics of this conductance are determined by a single gating variable $m(x,t)$ with activation function $m_\infty(V)$ and time constant τ_m. The equations governing the membrane potential $V(x,t)$ and the gating variable $m(x,t)$ along the cable are

$$\begin{aligned} \tau\frac{\partial}{\partial t}V(x,t) &= \lambda^2\frac{\partial^2}{\partial x^2}V(x,t) - (V(x,t)-E_L) \\ &\quad -\gamma_m\, m(x,t)\,(V(x,t)-E_m), \\ \tau_m\frac{\partial}{\partial t}m(x,t) &= m_\infty(V(x,t)) - m(x,t), \end{aligned} \tag{3}$$

where γ_m is the ratio of the maximal conductance of the active current to the leak conductance. In order to determine the perturbations to the oscillators we need to solve equation (3) with the oscillators at the ends of the cable as the oscillatory boundary conditions, determining the membrane potential at $V(0,t)$ and $V(l,t)$. For this, we first linearize equation (3) about the membrane voltage V_R around which the membrane potential oscillates, leading to the quasi-active approximation for the cable [10]. We can then show that the perturbation to oscillator $i = 1$ reads

$$p_1(t) \propto \frac{\partial}{\partial x}V(0,t) = \frac{Ab\,e^{i\omega t}}{\sinh(bL)}\left(e^{i\omega\theta_2} - \cosh(bL)\,e^{i\omega\theta_1}\right), \tag{4}$$

where

$$b = \sqrt{\gamma_R + \frac{\mu}{1+(\omega\tau_m)^2} + i\omega\left(\tau - \frac{\mu\,\tau_m}{1+(\omega\tau_m)^2}\right)}, \tag{5}$$

with $\gamma_R = 1+\gamma_m m_\infty(V_R)$ and $\mu = \gamma_m(V_R - E_m)\frac{\partial}{\partial V}m_\infty(V_R)$. Note that the active properties of the cable can be summarized by a single parameter, μ (see [11]). The sign of μ indicates whether the active conductance is regenerative ($\mu < 0$), restorative ($\mu > 0$), or passive ($\mu = 0$), where a regenerative current will amplify perturbations (e.g. a persistent sodium current), while a restorative current actively counteracts such perturbations (e.g. the hyperpolarization activated h-current).

We want to describe the evolution of the phase difference $\phi(t) = \theta_2(t) - \theta_1(t)$. For this we first need to determine the phase interaction function $H_i(\phi)$ that describes the average effect of perturbation $p_i(t)$ on the phase of oscillator i over a cycle of period $T = 2\pi/\omega$. For oscillator $i = 1$ this interaction function reads

$$H_1(\phi) = \frac{1}{T}\int_0^T Z(t)\,p_1(t+\phi)\,dt \tag{6}$$

$$= \frac{1}{2\omega}\rho\sin(\omega\phi + \xi) + \nu \tag{7}$$

where

$$\rho = \left|\frac{b}{\sinh(bL)}\right|, \tag{8}$$

$$\xi = \arg\left(\frac{b}{\sinh(bL)}\right), \tag{9}$$

and ν is a constant, and where $|z|$ is the absolute value and $\arg(z)$ is the angle of a complex number. Note that we use Andronov-Hopf oscillators with the iPRC given by $Z(t) = -\frac{1}{\omega A}\sin(\omega t)$. The interaction function $H_2(\phi)$ can be determined similarly and we obtain an equation describing the evolution of the phase difference between the two oscillators:

$$\dot{\phi} = -\varepsilon\frac{\rho}{\omega}\cos(\xi)\sin(\omega\phi). \tag{10}$$

The fixed points of this differential equation, i.e. where $\dot{\phi} = 0$, are thus $\omega\phi = k\cdot\pi$ where k is an integer. The stable fixed points are those points where $d\dot{\phi}/d\phi < 0$. The phase shift ξ is small for small L and ω, making the synchronous solution $\phi = 0$ stable.

Our goal is to determine the influence of the oscillator and cable parameters on how fast the phase-locking occurs. With the simplified system we can solve for $\phi(t)$ and obtain

$$\phi(t) = 2\arctan(c\exp(-t/\tau_l)), \tag{11}$$

where the phase-locking time constant $\tau_l = \omega/\varepsilon\rho\cos(\xi)$ and c depends on the initial conditions. Thus, ϕ approaches the stable solution exponentially with a time constant τ_l, when ϕ is sufficiently close to its fixed point. The approach will be slower than exponential when ϕ is further from the stable solution (see figure 1B).

Using the above results we can now illustrate the phase-locking time scales for this simplest possible oscillator configuration: two oscillators that are coupled via a passive or quasi-active cable. The two panels in figure 1C show how τ_l varies with the electrotonic distance L (with oscillator frequency $\omega/2\pi = 8$ Hz). For $L = 0$, the two oscillators are directly coupled and the locking is instantaneous. The time constant increases linearly with L for small L. Note that the active cable properties do not have a strong influence for distances up to $L = 1$. For larger L the regenerative current (i.e. $\mu < 0$) makes the locking faster than the passive or restorative currents. The panel on the right shows the same variables but with τ_l plotted on a log scale and for a larger range of L. Interestingly, there are values of L for which τ_l is infinite. This occurs at the moment that $\cos(\xi) = 0$, which is when the stable phase-locked solution changes from in-phase to anti-phase. For that exact value of L (which is at $L \sim 3$ for the cable with a regenerative current) there is not a single phase-locked solution. In general we can state that regenerative cable properties make the phase-locking dynamics faster. However, such a current also amplifies the dependence of ξ on L. As a consequence the phase-locked solution changes for smaller L and it is at these points that the phase-locking dynamics become very slow. Restorative conductances have precisely the opposite effect, typically making the phase-locking dynamics slower and decreasing the dependence of ξ on L.

Using our analysis, we can also see how synaptic conductance load onto the dendrites affects the locking dynamics of dendritic oscillators. We analyze such effects by adding a constant shunt to the cable. This is achieved in the model by varying R_m, which in turn affects the dendritic membrane time constant $\tau = R_m C_m$ and the electrotonic distance between the oscillators since $L = l/\lambda = l/\sqrt{R_m d/4R_a}$ (where l is the length of the cable, d is the diameter of the cable, R_a is the intracellular resistivity and C_m is the membrane capacitance). Increasing the shunt leads to decreases of R_m. As R_m approaches zero, L will go to infinity and τ will go to zero. As a consequence the time constant of locking goes to infinity. Conversely, an increase of R_m leads to a decrease of τ_l. We determined τ_l for typical dendritic cable parameters (figure 1D). We see a steep increase of τ_l as R_m decreases below 20 kΩ cm^2. Conversely, increasing R_m leads to a slow decrease of τ_l.

The above results show that in order for dendritic oscillators to phase-lock as slowly as possible, the oscillators typically should be located as distally from each other as possible. A consequence of such distal sources of the oscillations is that the amplitude of the oscillations at the soma will be attenuated. We can use our framework to infer the necessary amplitude of the dendritic oscillations in order

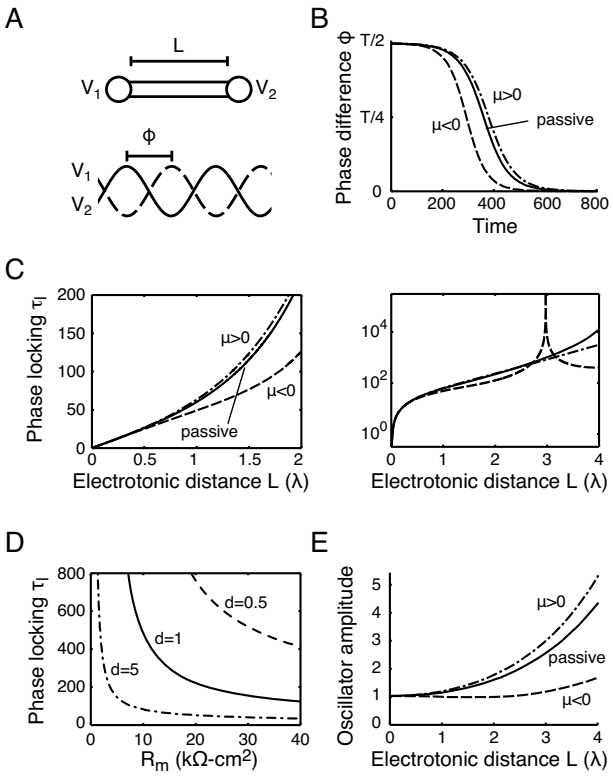

Figure 1. Phase-locking of two cable coupled oscillators. A: The two oscillators V_1 and V_2 with phase difference ϕ are coupled via a cable of electrotonic length L. B: Evolution of ϕ depends on the type of currents in the connecting cable. The oscillators have frequency $\omega/2\pi = 8$ Hz and are separated by a cable of $L = 1$. Cable properties are either passive, or active with a regenerative (dashed curve) or restorative current (dash dotted curve). The parameters of the regenerative and restorative currents are based on a h-type current and a persistent sodium current and are, respectively, $\mu = -1.5$, $\gamma_R = 1.2$ and $\tau_m = 1.1$ ms, and $\mu = 1.5$, $\gamma_R = 1.2$ and $\tau_m = 52$ ms. C: Time constant of phase-locking τ_l depends on cable properties. The two panels plot τ_l as a function of L for passive or active cables (see panel B). D: Dependence of τ_l on dendritic membrane resistance R_m for three different cable diameters d (in μm). The oscillator frequency is $\omega/2\pi = 8$ Hz. The cable is passive with length $l = 1000$ μm, membrane capacitance $C_m = 1\,\mu$F/cm^2, intracellular resistivity $R_a = 200\,\Omega$cm. E: Ratio of the dendritic and somatic oscillator amplitude as a function of the electrotonic distance L between the oscillators. Active cable parameters are as in panel B.

to match the experimentally determined amplitude of the oscillations at the soma of entorhinal stellate cells, which are in the order of 1–2 mV [4]. We can obtain explicit expressions of the amplitude of the dendritic oscillations as a function of the electrotonic distance between the oscillators. We assume that the soma is in the middle of the cable (at $x = l/2$), that it shows oscillations with amplitude A_s,

and that the two dendritic oscillators at the ends of the cable are synchronized (i.e. $\phi = 0$). The relation between the amplitude of the dendritic and the somatic oscillations is then $A = A_s\,|\cosh(bL/2)|$. In figure 1E we plot A as a function of the distance L between the oscillators. Typically, the dendritic oscillation amplitude needs to increase as L increases. However, when the connecting cable expresses a regenerative current, the amplitude of the dendritic oscillations can also be smaller than the somatic oscillation amplitude.

In summary, our mathematical analysis provides key requirements for a biophysical implementation of the interference model for grid fields. The biophysical model needs dendritic oscillators with a maximal electrotonic separation which can be achieved by distal locations of the dendritic oscillators and the presence of a shunt in the dendrites that connect the oscillators. The analysis also suggests that the interaction between the oscillators can be minimized by making use of the parameter regime in which the stable phase-locked state changes from in-phase to anti-phase, at which point τ_l is very large.

2.2 Biophysical Model

In the above weak coupling analysis, the phase-locking time constant τ_l was dependent on the small parameter ε. Since this was left as a free parameter we did not obtain absolute values for τ_l. We next use a biophysical implementation of the model to establish how fast phase-locking occurs for realistic parameter settings. Here we do not assume weak coupling between the oscillators, but add oscillations-generating conductances to the distal 150 μm ends of a passive cable with electrotonic length L (figure 2A). The subthreshold oscillations emerge from interactions between a persistent sodium current and a hyperpolarization activated h-current [6].

When we make the frequencies of the oscillating segments different – by providing input to one of the oscillators – we can observe interference patterns in the membrane potential halfway the cable (figure 2B). After removing the external input, however, the two oscillators return to their phase-locked configuration within ~ 2 seconds, which is reflected by the gradual increase of the amplitude of the interference pattern. Note again, that the interference mechanism for grid fields requires that the phase difference is maintained and should only change as a function of the external input.

As in the above analysis (see figure 1C), we determine how the phase-locking time constant τ_l scales with the electrotonic distance L between the oscillators (figure 2C). Simulations show that it is impossible to produce different oscillation frequencies for $L < 2$ since the oscillators are strongly locked. Hence, no interference patterns can be obtained for small L. For larger values of L it is possible to obtain different oscillation frequencies and we can see an approximately exponential increase of τ_l, reaching up to ~ 5 seconds when $L = 5$. Note that there is a range of values of L where τ_l is not defined (grey area in figure 2C). This corresponds to the parameter regimes in the above analysis where τ_l is infinite. However, in the conductance-based model we find varying values for τ_l, depending on the amplitude and timing of the external input to the oscillator. This means that the dynamics cannot be generically controlled for such parameters and suggests that minimal interactions between dendritic oscillators can only be obtained by maximal electrotonic separation.

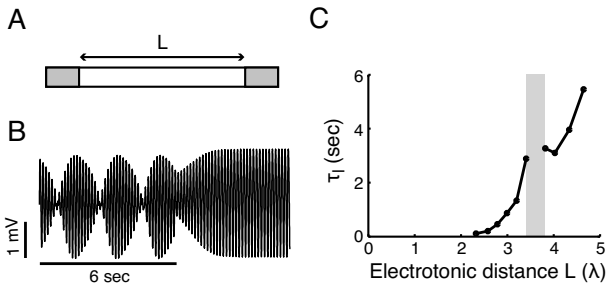

Figure 2. Phase-locking in a conductance based cable model. A: The ends of the cable (grey) contain the active conductances that generate the oscillations. The passive cable with electrotonic length L has membrane resistance $R_m = 10$ kΩ cm^2, intracellular resistivity $R_a = 200\,\Omega$cm and membrane capacitance $C_m = 1\,\mu$F/cm^2. B: Interference pattern of the membrane potential in the middle of the cable when providing input to one of the two oscillators for 6 seconds. The active segments of the cable are separated by $L = 3$. C: Phase-locking time constant of the cable model for different L. The grey area denotes a parameter range where τ_l is undefined.

3 Conclusion

Our analysis suggests a number of requirements for the interference framework to be implemented biophysically. We find that in order for grid fields to be formed by a single cell mechanism, the dendritic oscillators need to be electrotonically maximally removed from each other. At the same time we can determine the necessary dendritic oscillation amplitudes. Our analysis and simulations therefore provide key requirements that should be fulfilled by entorhinal stellate cells in order to show grid field activity via the single cell interference mechanism. Future work will explore whether the oscillator interactions can be sufficiently weak to maintain stable grid fields over extended periods of time.

Acknowledgements This work was supported by a Marie Curie Team of Excellence Fellowship (BIND MEXT-CT-2005-024831), the Gatsby Charitable Foundation, EU Framework 6 (IST-FET 1940), and the Hungarian National Office for Research and Technology (NAP2005/KCKHA005).

References

[1] T. Hafting, M. Fyhn, S. Molden, M.B. Moser, and E.I. Moser. Microstructure of a spatial map in the entorhinal cortex. *Nature*, *436*(7052):801–6, 2005.

[2] N. Burgess, C. Barry, and J. O'Keefe. An oscillatory interference model of grid cell firing. *Hippocampus*, *17*(9):801–12, 2007.

[3] M.E. Hasselmo, L.M. Giocomo, and E.A. Zilli. Grid cell firing may arise from interference of theta frequency membrane potential oscillations in single neurons. *Hippocampus*, *17*(12):1252–71, 2007.

[4] A.A. Alonso and R.R. Llinás. Subthreshold Na^+-dependent theta-like rhythmicity in stellate cells of entorhinal cortex layer II. *Nature*, *342*(6246):175–7, 1989.

[5] A.A. Alonso and R. Klink. Differential electroresponsiveness of stellate and pyramidal-like cells of medial entorhinal cortex layer II. *Journal of Neurophysiology*, *70*(1):128–43, 1993.

[6] C.T. Dickson, J. Magistretti, M.H. Shalinsky, E. Fransén, M.E. Hasselmo, and A.A. Alonso. Properties and role of I_{h} in the pacing of subthreshold oscillations in entorhinal cortex layer II neurons. *Journal of Neurophysiology*, *83*(5):2562–79, 2000.

[7] T. Hafting, M. Fyhn, T. Bonnevie, M.B. Moser, and E.I. Moser. Hippocampus-independent phase precession in entorhinal grid cells. *Nature*, *453*(7199):1248–52, 2008.

[8] L.M. Giocomo, E.A. Zilli, E. Fransén, and M.E. Hasselmo. Temporal frequency of subthreshold oscillations scales with entorhinal grid cell field spacing. *Science*, *315*(5819):1719–22, 2007.

[9] E.M. Izhikevich. *Dynamical Systems in Neuroscience: The Geometry of Excitability And Bursting*. Cambridge, MA: MIT Press, 2007.

[10] A. Mauro, F. Conti, F. Dodge, and R. Schor. Subthreshold behavior and phenomenological impedance of the squid giant axon. *Journal of General Physiology*, *55*(4):497–523, 1970.

[11] J.A. Goldberg, C.A. Deister, and C.J. Wilson. Response properties and synchronization of rhythmically firing dendritic neurons. *Journal of Neurophysiology*, *97*(1):208–19, 2006.